

# ChemComm

Accepted Manuscript



This is an *Accepted Manuscript*, which has been through the Royal Society of Chemistry peer review process and has been accepted for publication.

*Accepted Manuscripts* are published online shortly after acceptance, before technical editing, formatting and proof reading. Using this free service, authors can make their results available to the community, in citable form, before we publish the edited article. We will replace this *Accepted Manuscript* with the edited and formatted *Advance Article* as soon as it is available.

You can find more information about *Accepted Manuscripts* in the [Information for Authors](#).

Please note that technical editing may introduce minor changes to the text and/or graphics, which may alter content. The journal's standard [Terms & Conditions](#) and the [Ethical guidelines](#) still apply. In no event shall the Royal Society of Chemistry be held responsible for any errors or omissions in this *Accepted Manuscript* or any consequences arising from the use of any information it contains.

# Energy propagation throughout chemical networks

Thomas Le Saux,<sup>a,b,c</sup> Raphaël Plasson,<sup>\*d,e</sup> and Ludovic Jullien<sup>\*a,b,c</sup>

Received Xth XXXXXXXXXXXX 20XX, Accepted Xth XXXXXXXXXXXX 20XX

First published on the web Xth XXXXXXXXXXXX 200X

DOI: 10.1039/b000000x

**Living cells rely on chains of energy transfer involving functionally identified components and organizations to maintain their metabolism from an energy source. However, propagation of a sustained energy flux through a cascade of reaction cycles has only been recently reproduced at a steady state in simple chemical systems. As observed in living cells, the spontaneous onset of energy-transfer chains notably drives local generation of singular dissipative chemical structures: Continuous matter fluxes are dynamically maintained at boundaries between spatially and chemically segregated zones but in the absence of any membrane or predetermined material structure.**

## Introduction

The striking examples of function-driven organization and behavior of biological matter have continuously filled the dreams and motivated the works of chemists. Indeed, they provide obvious and challenging outcomes of interactions at the level of atoms and molecules. Natural products, biomolecules, cell membranes, etc., inspired key works, which ultimately led chemists to establish powerful structure-property relationships at the molecular and supramolecular levels. In contrast, several biological phenomena arising at the system level—integrating the interactions, the reactions, and the motions of the molecules—still escape understanding of chemists. It is precisely the purpose of Systems Chemistry to design and implement strategies aiming to reproduce them and extend their scope.<sup>1,2</sup>

At the system level, a living cell is indeed complex and rather counter-intuitive for a chemist. Beyond its composition (close to sea water for its inorganic components<sup>3</sup> but much more concentrated in organic molecules—about 0.3 mol.l<sup>-1</sup> in

E. Coli<sup>4</sup>), it is a highly heterogeneous (but deterministic) mixture of components (typically more than 10<sup>6</sup>) at concentrations covering an extremely wide 10<sup>-13</sup>-10<sup>-1</sup> mol.l<sup>-1</sup> range. More significantly, it is an autonomous out-of-equilibrium chemical system at steady-state.

Whereas the first feature is singular but deserves no more specific comment at that point, it is worth to make clear the implications of the second one. A mixture of reactants submitted to a chemical reaction evolves and relaxes toward chemical equilibrium. Once this state is reached, the system composition does not evolve anymore and the overall rate of each chemical reaction is null; this is known as the principle of detailed balance.<sup>5</sup> In contrast, the same reactive system in an out-of-equilibrium steady-state still exhibits constant concentrations but with values departing from equilibrium ones such that the overall rates of chemical reactions now remain non-vanishing. This breakdown of the detailed balance coupled to the steadiness of concentrations implies that all transformation fluxes—while being individually nonzero—globally cancel each others: nonequilibrium steady states must be maintained by cyclic processes.<sup>5</sup>

This last property implies that the concentrations in reactants and products are not anymore governed by the spontaneous chemical relaxation occurring in the system: at least one independent process (diffusion from a source or a sink, coupling with an external chemical reaction, photochemical reaction, ...) has to drive concentration values at a rate which is much larger than the spontaneous chemical relaxation. Since the system is maintained out-of-equilibrium with respect to the relaxing chemical reaction, it produces a flux of entropy. Therefore, beyond being fast enough, the driving process is necessarily energy-consuming: a living cell is a dissipative system, which is crossed by fluxes of energy.

Conversely it has been argued that the emergence, organization, and persistence of life on Earth could be interpreted in the light of energy fluxes.<sup>6-8</sup> Life, and in particular core biochemistry, could have acted as a relaxation channel that was driven into existence by primordial energy sources. Beyond its biological relevance, this attractive statement may provide a useful guideline for Systems Chemistry. Indeed it identifies key actors (an energy source, generalized catalysts<sup>9</sup>) and a scenario (assembling chains of energy transfer) to build min-

<sup>a</sup> École Normale Supérieure-PSL Research University, Department of Chemistry, 24, rue Lhomond, 75005 Paris, France. Tel: +33 1 44 32 33 33; E-mail: Ludovic.Jullien@ens.fr

<sup>b</sup> Sorbonne Universités, UPMC Univ Paris 06, UMR 8640 PASTEUR, F-75005, Paris, France.

<sup>c</sup> CNRS, UMR 8640 PASTEUR, F-75005, Paris, France.

<sup>d</sup> INRA, UMR408, Sécurité et Qualité des Produits d'Origine Végétale, F-84000 Avignon, France. Tel: +33 4 90 14 44 44; E-mail: raphael.plasson@univ-avignon.fr

<sup>e</sup> Université d'Avignon et des pays du Vaucluse, UMR408, SQPOV, 33 rue Pasteur, F-84029 Avignon cedex 1, France.

imal “living” cells.

In a chain of energy transfer (Fig. 1), an energy source drives a primary reaction cycle to a non-equilibrium state. The activated primary reaction cycle acts in turn as a secondary source, which transfers its free energy to secondary reaction cycles by coupling.<sup>10,11</sup> Further series of reaction cycles grafting events propagate energy throughout the whole network of chemical reactions. Maintaining continuous reaction cycles leads to two major energetic consequences: (i) Each reaction cycle possesses a nonzero free energy  $\Delta_r G$  and thus acts as a static reservoir of energy; (ii) Each reaction cycle is subject to nonzero reaction fluxes and thus acts as a dynamic source of entropy production.

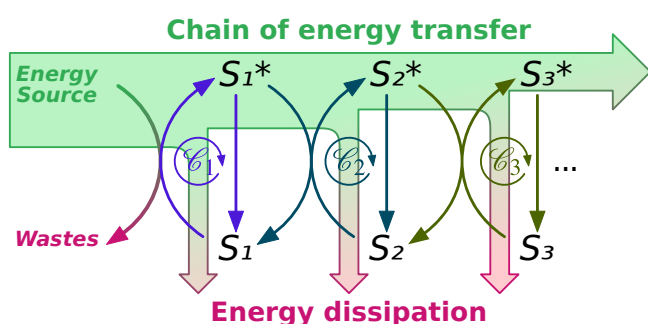


**Fig. 1** Onset and propagation of a chain of energy transfer. An external source of energy brings and maintains in an out-of-equilibrium state  $S_1^*$  the concentrations of a first subset of reactants. The continuous spontaneous relaxation from  $S_1^*$  back to the equilibrium state  $S_1$  leads to the emergence of a primary dissipative reaction cycle  $C_1$ . The activated state  $S_1^*$  is a putative secondary source of free energy. Thanks to coupling, it can bring a second subset of reactants to an out-of-equilibrium state  $S_2^*$ , which leads to transfer free energy to a secondary cycle  $C_2$  grafted on the primary one. As long as they satisfy the thermodynamic and kinetic constraints for coupling and free energy transfer, further series of reaction cycles grafting events can occur to propagate energy throughout a whole network of chemical reactions.

In fact the concept of chain of energy transfer provides a useful causal guideline to read out both the composition and the organization of a living cell. For example, in photosynthetic microorganisms, which relies on light, long-lived charge separation in photoactive transducers is primarily coupled with vectorial proton translocation across a membrane. Then the photogenerated electrochemical proton gradient is used by ATP-synthase as a secondary free energy source for ATP synthesis.<sup>12</sup> Thanks to enzymatic transducers, ATP hydrolysis subsequently drives the endergonic chemical reactions of the whole metabolism.

## Design of an energy transfer chain

In relation to designing a chain of energy transfer, driving a primary reaction cycle to a non-equilibrium state is not a difficult task. An assembly of reactants in a non-equilibrium state may directly be used as a primary source of chemical energy. Alternatively, chemists commonly use light or electric energy for molecular activation so as to shift reactive systems away from their state of thermal equilibrium. In contrast—and despite its ubiquity in biosystems—free energy transfer by means of coupled reactions does not presently belongs to the chemical repertoire.<sup>13,14</sup> Coupling two chemical reactions as such is not demanding: the realization of one reaction has to influence the occurrence of the second. The simplest way to couple two reactions is to rely on a same reactant. However such an approach is limited to coupling two reactions involving a same field of reactivity. In contrast, molecular transducers incorporating allosteric catalytic sites may couple reactions involving orthogonal reactivities.<sup>13</sup>

Hence, in living systems, reaction coupling involves transducers catalyzing orthogonal reactions (e.g., ATP-synthase coupling proton exchanges with esterification), shared “hub” reactants (e.g., ATP or NADH), and spatial matter exchanges (both active and passive matter transport occur in the heterogeneous cell environment<sup>15,16</sup>). The thermodynamic requirement for free energy transfer by means of coupled reactions is well-established: free energy dissipation associated to the spontaneous realization of the “driving” reaction pays for the occurrence of the endergonic reaction.<sup>10,11,17,18</sup> In contrast, the kinetic constraints governing the effective realization of the free energy transfer are not widely recognized: (i) To avoid free energy leakage, chemical relaxation associated to the realization of the “driving” reaction alone should be slower than chemical relaxation associated to the realization of the “driving” reaction coupled to the endergonic reaction; (ii) The rate constants associated to the realization of the “driving” reaction should be large enough so as to force the values of the control parameters of the endergonic reaction (“slave” reaction).<sup>13</sup> Biological energy-transfer chains exhibit such a thermokinetic hierarchy and are highly efficient for preventing the dissipation of energy as heat.

## Realizations of energy transfer chains

Two papers have recently reported independent efforts to build chains of energy transfer propagating energy throughout networks of chemical reactions at steady-state.<sup>19,20</sup> Both retained a simple design:

- A spatially distributed source of energy is applied;
- This results in the generation of concentration gradients;

- Several chemical reactions involving the same reactants and products are differently driven depending on the spatial position;
- Spatially extended cycles of chemical reaction and mass transport fluxes are eventually established.<sup>6–8</sup>

This results in spatial dynamic self organization (Fig. 2).<sup>21</sup> In particular, at the spatial scale where matter transport is faster than chemical relaxation, mass transport drives local concentrations out-of-chemical equilibrium (“chemical slavery” principle<sup>13</sup>) and energy can propagate throughout coupled reaction cycles as well as in space.

Although without metabolic closure—as they still rely on preexisting non-self-synthesized compounds<sup>22</sup>—the investigated networks of chemical reactions consume, propagate and use energy for organizational purposes. Moreover, since observations are performed in open microsystems at steady-state, the experimental design is compatible with high-throughput screening the composition of the external medium as well as the application of further constraints to generate more complex dynamic behaviour.

### Polymerization in a thermal gradient

In a recent paper, D. Braun *et al*<sup>20</sup> address the dynamic emergence of biopolymers in a diluted world. Indeed biopolymers are presently the vital building blocks of all known life forms. However spontaneously forming one of their bonds typically requires monomer concentrations above the millimolar range. How significantly “long” biopolymers (e.g. self-replicating ribozymes) could have originally emerged in the absence of concentrated soup of monomers? D. Braun *et al* have introduced and experimentally demonstrated a mechanism to bridge this gap: the escalated polymerization of oligonucleotides by a spatially confined thermal gradient, which would be typically observed in porous materials of hydrothermal vents (Fig. 3).

The gradient first accumulates oligonucleotide monomers by thermophoresis and convection. In the zone of largest monomer concentration, reversible monomer polymerization occurs by means of pairing of complementary sequences. At their turn, the polymers are locally trapped by thermophoresis and convection retaining longer polymers exponentially better. Thus polymerization and accumulation become mutually self-enhancing and result in a hyperexponential escalation of polymer length. Taking into account the thermophoretic properties of RNA, D. Braun *et al* suggest that a pore length of 5 cm and a temperature difference of 10 K over 100  $\mu\text{m}$  width is sufficient to locally polymerize 200-mers of RNA in micromolar concentrations from a highly dilute solution of monomers (nanomolar concentration). Under such conditions, the probability to generate these long RNAs is raised by an impressive

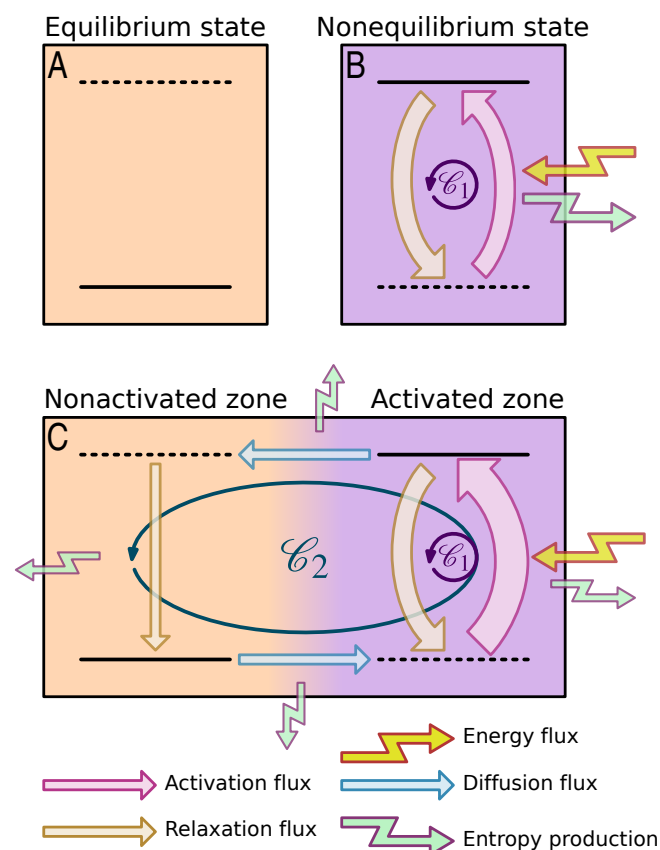


**Fig. 2** Design of a chain of energy transfer resulting from spatially heterogeneous activation. **A:** At equilibrium, each reaction of a reactive network is detailed balanced; reactant concentrations are at their equilibrium values and no reaction flux is sustained. **B:** When connected to an energy source, non-detailed balance reactions can be maintained, establishing a primary dissipative reaction cycle  $C_1$  that drives reactant concentrations out-of-equilibrium and continuously produces entropy. **C:** A physical connection between equilibrated and activated systems locally generates an extended cycle  $C_2$ , which involves reactions and mass transport, propagating the energy flux in space and delocalizing the entropic dissipation. A similar phenomenon arises when matter transports rather than chemical reactions are activated (see Fig. 4), or when two differently activated systems are connected (see Fig. 6).

$> 10^{600}$  factor compared with polymerization in a chemical equilibrium.

The chain of energy transfer generated in the preceding system is most easily evidenced by considering the thermogenerated concentration map within the pore (Fig. 4). In the absence of any thermal gradient, monomer concentration is vanishing and homogenous within the pore. In contrast, the forced temperature gradient is a source of free energy able to generate and maintain concentration gradients. As a consequence, monomer concentration (and thus chemical potential) is con-

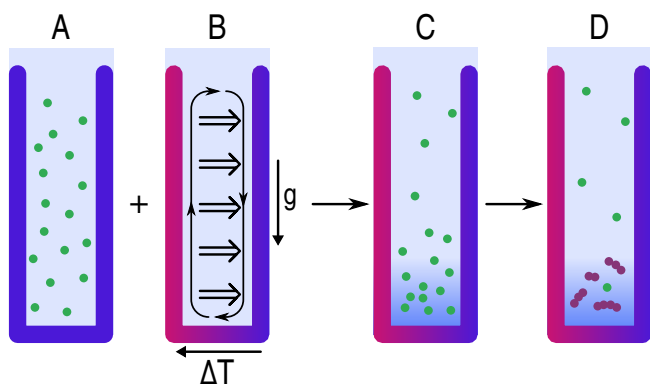


**Fig. 3** Local endergonic polymerization in a thermal gradient. **A:** A water-filled pore is open at the top and exposed to a solution of monomers engaged in a reversible reaction of polymerization. At monomer concentrations much below the dissociation constant, polymerization is thermodynamically disfavored: no significant amount of polymer is formed in the system at constant temperature. **B:** This situation markedly changes when the pore is subjected to a spatially confined horizontal temperature gradient. The temperature gradient drives thermal convection ( $\rightarrow$ ) originating from the thermal expansion of water at the hot side. Additionally, the monomers and any formed polymer move from hot to cold via thermophoresis ( $\Rightarrow$ ). **C:** As a consequence of the combination of both effects, the monomers are accumulated at the pore bottom, exponentially dependent on the molecule length at optimal trap width. **D:** As a result of locally enhancing concentrations, high molecular weight polymers are formed at the pore bottom. The figure is inspired from Fig. 1 in reference<sup>20</sup>.

siderably increased at the pore bottom so as to start to significantly generate polymers as a spontaneous chemical relaxation; this generates a first dissipative cycle  $C_1$ . Polymers will themselves be trapped at the pore bottom, guarantying their thermodynamic stability, but a small quantity will eventually reach the top of the pore. Due to their high dilution there, this small excess of polymer will in turn spontaneously relax by depolymerization, releasing back the monomers; this constitutes a secondary cycle  $C_2$ . The full set of these processes consists in a large chemical reaction/mass transport cycle  $C_3$ : monomers are transported to the pore bottom where they get polymerized, polymers are transported to the top of the pore where they get hydrolyzed, and so on in a continuous cyclic flux.

From a dynamic point of view, two different processes can be distinguished. At first, a progressive polymerization and accumulation of the resulting polymers will be performed. This is a chemical flux that can only be vanishing, until the steady state is reached. From an energetic point of view, this process is an energy storage, as polymers that would not be stable in the absence of the temperature gradient are synthesized and accumulated. Then, a large cycle of monomer

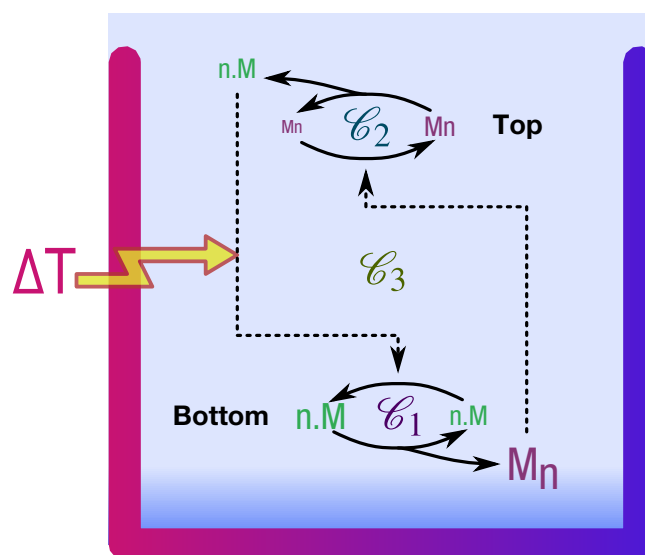


**Fig. 4** Reactive and transport processes occurring from polymerization in a thermal gradient. The thermal gradient generates the motion of the monomers leading to the formation of a concentration gradient with largest concentration at the pore bottom, driving the formation of polymers. It results in the activation of a primary dissipative reaction cycle  $C_1$ . Despite enhanced trapping with respect to monomers, a small part of the polymer molecules eventually arrives at the pore top where they spontaneously depolymerize, yielding to locally replenish in monomers. It results in the activation of a secondary dissipative reaction cycle  $C_2$ . The resulting unbalance between the top and the bottom of the pore cause activation of an extended reaction-convection cycle  $C_3$  similar to a pump transporting monomers from the top to the bottom zone and polymers from the bottom to the top zone. The relative reactant concentrations are related to the font sizes. Solid arrows represent the local fluxes, and dashed arrows show the mass transports.

transport/polymerization/polymer transport/depolymerization is progressively established. Eventually, this large cycle will be non-vanishing at steady state, dissipating the consumed energy.

The preceding reaction-convection cycle is not the sole process active to dissipate energy. In fact convection alone leads to a large entropy production and may become the major dissipative process. However, the significance of this cyclic process should not be underestimated in the present context, especially when polymerizing different monomers, as for example to form RNA from nucleotides. In the absence of this cycle, polymerization reactions would be strictly at chemical equilibrium in each of the pore zones. As a consequence, it would result in a combinatorial mixture of polymers exhibiting an equilibrium distribution. In contrast, in the presence of an active reaction-convection cycle, an excess of polymerization occurs at the pore bottom, and an excess of depolymerization

takes place at the pore top. The two opposite reactions are performed in different conditions, which drives an *irreversible* polymerization/depolymerization process, that actively generates polymers at steady-state. Interestingly, this is also a *sine qua non* condition to form polymers exhibiting sequences escaping thermodynamic disorder.<sup>23</sup> As a consequence, optimizing the establishment of the dissipative cycle would be a way to maximize the probability for the emergence of non-trivial sequences.

### Conversion of light into chemical energy

Inspired by photosynthesis, in which visible-light absorption ultimately shifts the hydrolysis of colorless ATP (giving rise to colorless ADP and inorganic phosphate) out of equilibrium, Jullien *et al* have introduced a mechanism in which light can locally set out-of-chemical equilibrium a reaction involving “blind” reactants. The design of their chain of energy transfer relies on a transducer (2-hydroxy-3,5,6-trichloro-azobenzene, further referred as HTCAB, a photoacid which becomes more acidic upon light absorption), for which light absorption leads to energy storage upon conversion to a state of higher free energy, and a “hub” reactant (the proton). A patterned illumination was applied to a liquid solution of the reversible photoacid which becomes more acidic upon light absorption.<sup>24,25</sup> It resulted in the formation of an acidic well at steady-state. To propagate this light-powered primary spatial organization and increase its complexity, Jullien *et al* introduced slow proton-exchanging components ( $\text{CO}_2(\text{soln})/\text{HCO}_3^-$ ), which got coupled with the primary driving reactions. As a result, they photogenerated non-trivial nonmonotonic proton concentration profiles in a steady-state (Fig. 5).

Without light, the relative proportions in the acidic and basic states of T and C stereoisomers are governed by thermally-driven exchange processes. In particular, the solution pH is fixed by T, which is the only stereoisomer existing at chemical equilibrium.

Light induces photoisomerization between the cis and trans stereoisomers of HTCAB (noted respectively C and T), each of them existing in either a protonated and a deprotonated state (noted respectively TH and T<sup>-</sup> for T, CH and C<sup>-</sup> for C).<sup>24,26</sup> Light drives the realization of four new exchange processes: TH → CH, CH → TH, T<sup>-</sup> → C<sup>-</sup>, and C<sup>-</sup> → T<sup>-</sup>. This leads to steady states with a T/C ratio that depends on the irradiation wavelength. Namely, UV irradiation tends to favor the formation of the cis stereoisomer, while blue irradiation the trans stereoisomer.

Due to the difference of proton exchange properties of the stereoisomers, irradiation is accompanied by a more complex chemical process. During a transient regime, global conversion of trans to cis compounds T → C leads to initially establish an acidification flux, which is progressively challenged

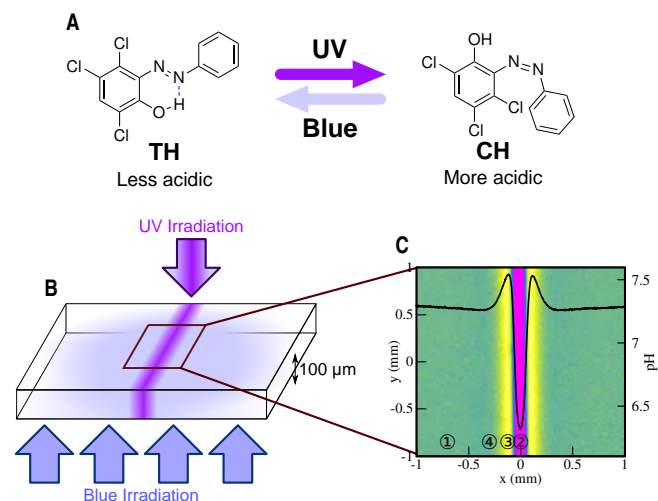


**Fig. 5** Evidence for conversion of light into chemical energy. **A:** Photoisomerization of HTCAB. In the trans stereoisomer TH, acidity is diminished by the hydrogen bond between the phenol and an azo nitrogen, whereas in the cis configuration CH the hydrogen bond is lost, restoring the intrinsic acidity of the substituted phenol. UV and blue illuminations respectively favor cis and trans stereoisomers; **B:** UV (40.5  $\mu\text{m}$ -wide Gaussian 375 nm light sheet) and blue (uniform at 480 nm) illumination pattern applied on 100  $\mu\text{m}$ -thin solution layer containing HTCAB, and Fluorescein as a fluorescent pH reporter; **C:** Experimental pH maps at steady-state retrieved from the 2 mm  $\times$  2 mm epi-fluorescence microscopy field of view upon submitting an atmosphere-equilibrated  $3.0 \cdot 10^{-4}$  M HTCAB and  $1.25 \cdot 10^{-6}$  M Fluorescein solution in water:acetonitrile 1:1 (v/v) to a UV + blue illumination with respective photon fluxes  $I_0(375) = 8.810 \cdot 10^{-2} \text{ Ein} \cdot \text{s}^{-1} \cdot \text{m}^{-2}$  and  $I_0(480) = 7.910 \cdot 10^{-3} \text{ Ein} \cdot \text{s}^{-1} \cdot \text{m}^{-2}$  at T=298 K. The zones ①–④ are indicated in reference to Fig. 6C.

by a reverse alcalinization flux C → T, as C accumulates. At steady state, the continuous deprotonation flux of CH is balanced by the continuous protonation flux of T<sup>-</sup> (see Fig. 6A). Thus a primary light-sustained dissipative cycle  $C_1$  is activated. In the resulting steady-state, the set of concentrations {TH, T<sup>-</sup>, CH, C<sup>-</sup>, H<sup>+</sup>} differs from the one at chemical equilibrium; in particular CH and C<sup>-</sup> are photogenerated and the solution becomes more acidic than without illumination. The acidification extent is thus significantly dependent on the irradiation wavelength, as a function of the steady-state value of the T/C ratio. Whereas a large acidification is eventually obtained with UV irradiation that favours the formation of C states, a weak acidification is obtained with blue irradiation that favours the formations of T states (Fig. 5).

The experiments have been performed in presence of a nonuniform irradiation: a thin UV stripe is applied in a uniformly blue-irradiated system (see Fig. 5B). As a consequence, each zone leads to different steady state concentra-

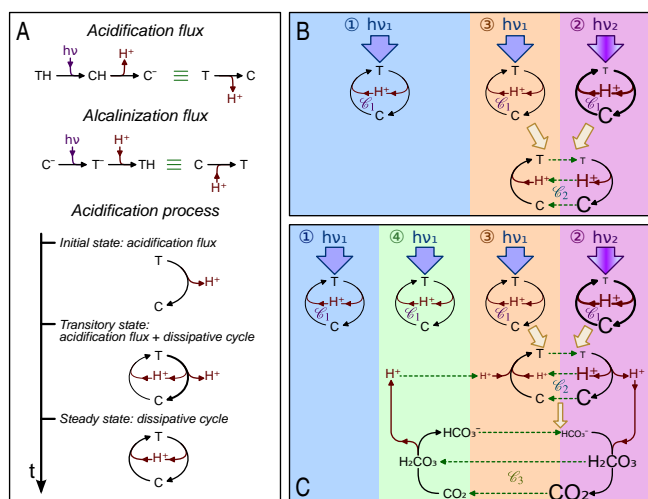


**Fig. 6** Reactive and diffusive processes occurring from irradiating HTCAB solutions. **A:** Homogeneous illumination drives both acidification and alcalinization fluxes associated to HTCAB photoisomerization. During an acidification process upon T irradiation, the initial acidification flux is progressively compensated by an alcalinization process; after a transient regime of acidification, light sustains a primary dissipative reaction cycle  $C_1$  at steady state. **B:** With the patterned illumination, different steady-states are reached by  $C_1$  in the blue- (①) and UV- (②) illuminated zones. The resulting concentration gradients at the corresponding boundary (③) cause photo-activation of an extended reaction-diffusion cycle  $C_2$  similar to a proton pump transporting protons from the blue- to the UV-illuminated zone. **C:** In the presence of dissolved  $\text{CO}_2$ , further proton exchanges involving  $\text{CO}_2$ -derived species get driven by the proton pump, which cause the emergence of a tertiary reaction-diffusion cycle  $C_3$ . Due to the slow hydration of dissolved  $\text{CO}_2$ , proton release from  $\text{H}_2\text{CO}_3$  ionization takes place beyond the location of the proton pump (zone ④), generating basic wings on the side of the pH well as seen in Fig. 5C. The relative reactant concentrations in the zones ③ and ④ are related to the font sizes. Full arrows represent the chemical fluxes and dotted arrows the chemical diffusions.

tions, more acidic in the UV-irradiated zone than in the blue-irradiated zone. This results in concentration gradients, especially abrupt at the sharp boundary between the blue and UV illuminated zones (e.g. the concentration in  $\text{H}^+$  is multiplied by ten over a distance of few tens of  $\mu\text{m}$ ). Concentrations are here not anymore solely governed by the light-sustained photochemical and proton exchanges, but as well by the relaxation matter fluxes induced by diffusion. In contrast to the situation encountered at steady-state with a homogeneous illumination (Fig. 6A), the continuous CH-deprotonation and  $\text{T}^-$ -protonation fluxes now only partially cancel each other. It results in the generation of a continuous deprotonation flux of HTCAB—related to a proton source—in the UV-irradiated

zone, and a continuous protonation flux—related to a proton sink—in its periphery (Fig. 6B). Thus a spatially-segregated photocycle of reaction-diffusion  $C_2$  involving protons as well as HTCAB compounds emerges at the boundary of the UV-irradiated zone. It can be compared to a membrane-free photodriven proton pump<sup>27</sup> working at a steady-state, in which protons are continuously pumped from the blue- to the UV-illuminated zone. This process counteracts the spontaneous proton diffusion from the UV- to the blue-illuminated zone, and avoids excessive widening of the pH pattern.

This photogenerated reaction-diffusion dissipative cycle can be coupled further in presence of other acidobasic couples. Namely, in the presence of carbon dioxide-derived species, in the UV-irradiated area—where protons release is driven by the proton pump—there is a continuous protonation flux transforming  $\text{HCO}_3^-$  into  $\text{H}_2\text{CO}_3$  and dissolved  $\text{CO}_2$ . In its remote periphery,  $\text{CO}_2$  hydration leads to release protons and  $\text{HCO}_3^-$  from  $\text{H}_2\text{CO}_3$ . As a consequence, a tertiary reaction-diffusion cycle  $C_3$  emerges, branched onto the secondary one  $C_2$ .

An interesting property of the  $\text{CO}_2/\text{HCO}_3^-$  acidobasic couple is its slow kinetics—in link with the slow  $\text{CO}_2$  hydration. This implies that the relaxation process by diffusion counteracting the nonequilibrium acidobasic processes is performed over a larger distance than the one involving HTCAB compounds:  $C_3$  propagates much farther than  $C_2$  (Fig. 6C). The photocycle of reaction-diffusion  $C_2$  does not spatially extend much beyond the close periphery of the UV-irradiated zone, as the proton exchange kinetics involving C/T compounds are very fast. In contrast, the  $\text{H}_2\text{CO}_3$  molecules generated by fast protonation of  $\text{HCO}_3^-$  in the UV-irradiated zone do not have enough time to locally dehydrate and yield  $\text{CO}_2$ ; hence  $\text{H}_2\text{CO}_3$  locally accumulates with respect to  $\text{CO}_2$ . Conversely, in the close periphery of the UV-illuminated zone, the  $\text{CO}_2$  molecules cannot regenerate the consumed  $\text{H}_2\text{CO}_3$  fast enough to locally reach the thermodynamic regime;  $\text{CO}_2$  thus accumulates with respect to  $\text{H}_2\text{CO}_3$ . Hence, the  $C_3$  cycle is active at a significantly large distance associated to the slow  $\text{CO}_2$  hydration, while the extent of the  $C_2$  cycle is typically limited by the distance associated to the relaxation of the blue light-driven  $\text{TH}_2\text{Cl}_3$  photo-isomerization.

The coexistence of two proton exchange dissipative cycles of different spatial extension is revealed by a singular pH map as seen in Fig. 5C. As shown in Fig. 6C, the proton pump  $C_2$  continuously pumps protons from the close proximity of the UV-illuminated zone (zone ③) to the UV illuminated zone (zone ②). In contrast, the reaction-diffusion cycle  $C_3$  continuously pumps protons from the UV-illuminated zone (zone ②) to the remote periphery of the UV-illuminated zone (zone ④). The spatial desynchronization of the two cycles leads to a  $\text{H}^+$  deficit interval, resulting in the generation of a pH well circumvented by two wings as observed experimentally.

Here again, this process is characterized by both storage and

dissipation of chemical energy. Far from the UV-illuminated zone where illumination is homogeneous, only the primary cycle  $C_1$  participates to light energy dissipation by maintaining HTCAB concentrations at non-equilibrium values. There,  $C_1$  is futile and not coupled. In this zone, chemical energy is solely stored in the nonequilibrium T/C ratio, in direct relationship with the photochemical reaction.

In contrast, in the UV-illuminated zone and at its borders, energy dissipation gives additionally rise to dissipative reaction-diffusion cycles of various spatial extension, coupled one to each other in a chain of energy transfer. Effective energy is transferred from light to not only the T/C compounds, but also to the  $\text{CO}_2$ -derived species, as well as under the form of steady concentrations gradients. The nonequilibrium state of  $\text{CO}_2$  is revealed by computing for all the chemical reactions the spatial dependence of  $\Delta_r G = RT \ln(Q_r(x)/K_r)$ , where  $Q_r(x)$  and  $K_r$  designate respectively the local concentration quotient and the thermodynamic constant associated to the reaction  $r$ . At any position, the system proved to be essentially at local chemical equilibrium with regards to all the reactions except ionization of dissolved carbon dioxide in the UV-irradiated zone and at its borders. For this reaction, whereas  $Q$  is equal to 40% of  $K$  in the UV-illuminated zone, it rises up to 160% of  $K$  in its periphery. Hence the ratio  $[\text{H}_3\text{O}^+] \times [\text{HCO}_3^-]/[\text{CO}_2]$  varies by a factor 4 around its equilibrium value over 100  $\mu\text{m}$ . A notable quantity of chemical energy originating from light eventually got stored as nonequilibrium concentrations of dissolved  $\text{CO}_2$ .

## Concluding remarks

On the basis of two experimental systems summed up in Table 1, the preceding paragraphs converge to validate the relevance of patterning energy sources on which reaction cycles are grafted to generate and sustain at steady-state chains of energy transfer in abiotic systems. Grafting a reversible polymerization reaction involving an oligonucleotide monomer onto a patterned temperature profile locally drove the formation of an endergonic polymer and a continuous dissipative polymerization/depolymerization process. Grafting a reversible photoacid and proton exchange reactions onto a patterned illumination profile led to establish a spatially extended proton pump, and to locally depart from its equilibrium a reaction in which reactants and products do not absorb light. In fact, sustaining reactive systems out of equilibrium at steady state is an essential prerequisite to reproduce some of the most attractive dynamic features of biochemical systems<sup>13</sup> as well as to benefit from a significant kinetic window to experience Darwinian evolution in a chemical world.<sup>28</sup>

It is worth to emphasize that multiple energy sources are relevant to generate and sustain at steady-state chains of energy transfer. Temperature gradients and light have been used

to introduce diffusion-mediated frustrations in the two experimental systems presented above. However it exists numerous alternative approaches (for instance relying on microsystems or microelectrodes) to drive spatial concentrations of reactants down to the micrometer scale in a medium in which diffusion is active.<sup>29–32</sup>

Energy sources patterning associated to reaction cycles grafting are also directly relevant to engineer “chemical entities”<sup>33</sup> which may emerge and sustain, provided that their “protometabolism” can extract and propagate energy from the medium. Interestingly, in both systems reported above, the onset of the chains of energy transfer was notably accompanied by the emergence of two constitutive features of living systems: (i) medium-dependent (phenotypic) expressions of singular spatial distributions of matter and (ii) local sustainability of non-vanishing reaction fluxes.

It now remains to extend the principle of energy propagation and coupling chemical cycles to new types of chemistries. Non-covalent associations<sup>34</sup> as well as polymerization reactions<sup>35</sup> could be particularly attractive to introduce nonlinearities. Indeed, further biologically-relevant phenomena leading to highly complex organizations are expected from grafting reaction cycles introducing feedbacks on the former cycles (Fig. 1).

## References

- 1 R. F. Ludlow and S. Otto, *Chem. Soc. Rev.*, 2008, **37**, 101–108.
- 2 K. Ruiz-Mirazo, C. Briones and A. de la Escosura, *Chem. Rev.*, 2014, **114**, 285–366.
- 3 D. H. Evans, *Osmotic and Ionic Regulation: Cells and Animals*, CRC Press Inc, Boca Raton, 2009.
- 4 B. D. Bennett, E. H. Kimball, M. Gao, R. Osterhout, S. J. V. Dien and J. D. Rabinowitz, *Nat. Chem. Biol.*, 2009, **5**, 593–599.
- 5 M. J. Klein, *Phys. Rev.*, 1955, **97**, 1446–1447.
- 6 H. Morowitz and E. Smith, *Complexity*, 2007, **13**, 51–59.
- 7 R. Pascal and L. Boiteau, *Phil. Trans. Roy. Soc. B: Biol. Sci.*, 2011, **366**, 2949–2958.
- 8 R. Braakman and E. Smith, *Phys. Biol.*, 2013, **10**, 011001.
- 9 M. Eigen and P. Schuster, *The hypercycle, a principle of natural self-organization*, Springer, Berlin, 1979.
- 10 A. Katchalsky and P. F. Curran, *Nonequilibrium Thermodynamics in Biophysics*, Harvard University Press, Cambridge, 1965.
- 11 T. L. Hill, *Free energy transduction in biology, the steady-state kinetic and thermodynamic formalism*, Academic Press, New York, 1977.
- 12 P. Mitchell, *Eur. J. Biochem.*, 1979, **95**, 1–20.
- 13 L. Jullien, A. Lemarchand, S. Charier, O. Ruel and J.-B. Baudin, *J. Phys. Chem. B*, 2003, **107**, 9905–9917.
- 14 D. Soloveichik, G. Seelig and E. Winfree, *Proc. Natl. Acad. Sci. USA*, 2010, **107**, 5393–5398.
- 15 B. N. Kholodenko, *Nat. Rev. Mol. Cell. Biol.*, 2006, **7**, 165–176.
- 16 S. Soh, M. Byrská, K. Kandere-Grzybowska and B. A. Grzybowski, *Angew. Chem. Int. Ed.*, 2010, **49**, 4170–4198.
- 17 S. Lems, H. J. van der Kooij and J. de Swaan Arons, *Chem. Eng. Sci.*, 2003, **58**, 2001–2009.
- 18 R. Plasson and A. Brandenburg, *Origins of Life and Evolution of Biospheres*, 2010, **40**, 93–110.

**Table 1** Characteristics of the systems of thermophoretic polymerization<sup>20</sup> and light-pattern controlled acidification.<sup>19</sup>

	Thermophoretic polymerization	Light-pattern controlled acidification
Energy source	Temperature gradient	UV/blue irradiation
Direct effect	Concentration gradients	Local nonequilibrium T/C ratio
Primary relaxation	Polymerization	Proton exchanges
Primary cycle	Polymerization cycle at the pore bottom	Proton pump at UV boundary
Secondary cycle	Mass transport cycle between the top and the bottom	H <sup>+</sup> -pump feeded carbonate cycle
General feature	Delocalized cycle of polymerization/depolymerization	Long distance H <sup>+</sup> transportation by CO <sub>2</sub>

- 19 M. Emond, T. L. Saux, J.-F. Allemand, P. Pelupessy, R. Plasson and L. Jullien, *Chem. Eur. J.*, 2012, **18**, 14375–14383.
- 20 C. B. Mast, S. Schink, U. Gerland and D. Braun, *Proc. Natl. Acad. Sci. USA*, 2013, **110**, 8030–8035.
- 21 N. Lane, J. F. Allen and W. Martin, *BioEssays*, 2010, **32**, 271–280.
- 22 B. H. Weber, *Ann. NY Acad. Sci.*, 2000, **901**, 132–138.
- 23 D. Andrieux and P. Gaspard, *Proc. Nat. Acad. Sci. USA*, 2008, **105**, 9516–9521.
- 24 M. Emond, T. L. Saux, S. Maurin, J.-B. Baudin, R. Plasson and L. Jullien, *Chem. Eur. J.*, 2010, **16**, 8822–8831.
- 25 M. Emond, J. Sun, J. Gregoire, S. Maurin, C. Tribet and L. Jullien, *Phys. Chem. Chem. Phys.*, 2011, **13**, 6493–6499.
- 26 P. Haberfeld, *J. Am. Chem. Soc.*, 1987, **109**, 6177–6178.
- 27 P. Haberfeld, *J. Am. Chem. Soc.*, 1987, **109**, 6178–6179.

- 28 R. Pascal, A. Pross and J. D. Sutherland, *Open Biol.*, 2013, **3**, 2046–2441.
- 29 C. Amatore, F. Bonhomme, J.-L. Bruneel, L. Servant and L. Thouin, *J. Elec. Chem.*, 2000, **484**, 1–17.
- 30 H. Wu, B. Huang and R. N. Zare, *J. Am. Chem. Soc.*, 2006, **128**, 4194–4195.
- 31 S. K. W. Dertinger, D. T. Chiu, N. L. Jeon and G. M. Whitesides, *Anal. Chem.*, 2001, **73**, 1240–1246.
- 32 J. Olofsson, H. Bridle, J. Sinclair, D. Granfeldt, E. Sahlin and O. Orwar, *Proc. Natl. Acad. Sci. USA*, 2005, **102**, 8097–8102.
- 33 A. Lemarchand and L. Jullien, *J. Phys. Chem. B*, 2004, **108**, 11782–11791.
- 34 R. Plasson and Y. Rondelez, *Multiscale Analysis and Nonlinear Dynamics: From Genes to the Brain*, 2013, pp. 113–145.
- 35 R. Plasson and H. Bersini, *J. Phys. Chem. B*, 2009, **113**, 3477–3490.

Relaxed Mass Transport

Activated Reaction

Relaxed Reaction

Activated Mass Transport

